

## LETTERS

### Shape Transformation and Surface Melting of Cubic and Tetrahedral Platinum Nanocrystals

Zhong L. Wang\*

*School of Materials Science and Engineering, Georgia Institute of Technology, Atlanta, Georgia 30332-0245*

Janet M. Petroski, Travis C. Green, and Mostafa A. El-Sayed\*

*Laser Dynamics Laboratory, School of Chemistry and Biochemistry, Georgia Institute of Technology, Atlanta, Georgia 30332-0400*

*Received: March 24, 1998; In Final Form: June 2, 1998*

We report transmission electron microscopic studies of in-situ temperature-induced shape transformation and melting behavior of polymer-capped cubic and tetrahedral nanocrystals. Our results indicate that the surface-capping polymer is removed by annealing the specimen at temperatures between 180 and 250 °C. The particle shapes show no change up to ~350 °C. In the temperature range between 350 and 450 °C, a small truncation occurs in the particle shapes but no major shape transformation is observed. The particle shapes experience a dramatic transformation into spherical-like shapes when the temperature is raised above ~500 °C, where surface diffusion or surface premelting (softening) takes place. Above 600 °C, surface melting becomes obvious leading to coalescence of the surfaces of neighboring nanocrystals and a decrease in the volume occupied by the assembled nanocrystals. The surface melting forms a liquid layer a few atomic layers deep around the still solid core of the nanocrystal. This temperature is much lower than the melting point of bulk metallic platinum (1769 °C). The reduction in the melting temperature is discussed in terms of the surface tension of the solid–liquid interface ( $\gamma_{SL}$ ). For an 8 nm diameter Pt nanocrystal,  $\gamma_{SL}$  is calculated to be 2.0 N m<sup>-1</sup> at 650 °C, which is smaller than that of the bulk solid–vapor metal surface tension ( $\gamma_{SV}$ ). This reduction is proposed to be due to the compensation of the increase in  $\gamma_{SV}$  of the nanocrystal by the wetting effect at the solid–liquid interface.

#### 1. Introduction

Platinum nanocrystals with a high percentage of cubic-, tetrahedral-, or octahedral-like shapes have been synthesized by our group using a colloidal method.<sup>1,2</sup> In this synthesis, the shapes of the Pt nanocrystals are controlled by changing the ratio of the concentration of capping polymer (polyacrylate) to that of K<sub>2</sub>PtCl<sub>4</sub> being reduced by H<sub>2</sub> at room temperature. This has opened a new direction for catalysis. Not only is the

catalytic activity dependent on the size<sup>3</sup> but it can also depend on the shape of the nanocrystals. However, for efficient catalysis, the capping polymer needs to be removed. Furthermore, many catalytic reactions take place at elevated temperatures. Thus, future applications would require heating the catalyzed reaction mixture. It is thus necessary to determine the temperatures at which the capping polymer is removed and the thermal stability of these nanocrystals with respect to shape changes and melting. This is the focus of this study.

Several questions are raised in this present study: (1) How high does the annealing temperature need to be to remove the

\* Corresponding authors.

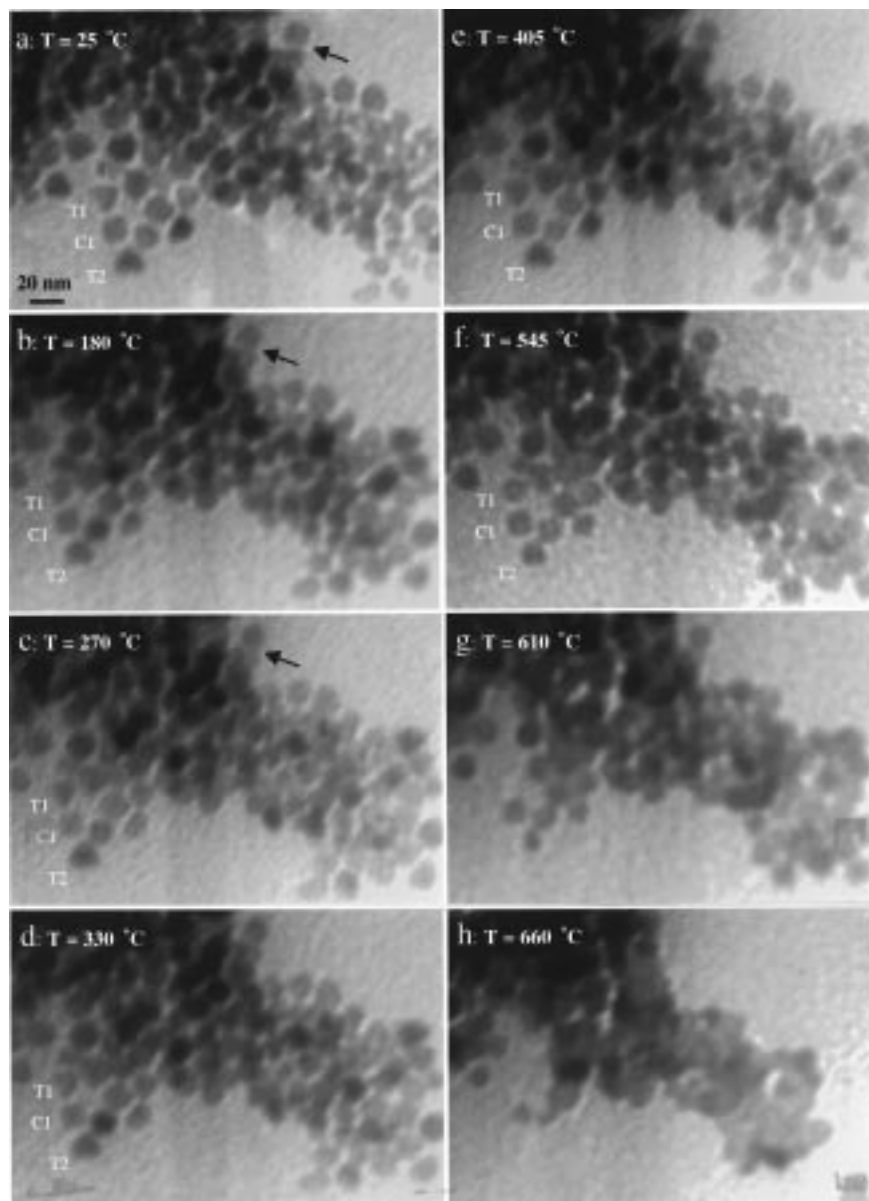


**Figure 1.** In-situ TEM images recorded from the same area of capped Pt nanocrystals at various specimen temperatures, showing the evaporation of capping polymer, coalescing, and macroscopic melting of Pt nanocrystal agglomeration (see text). The temperature for the images was sensed by a thermocouple attached to the thermal cup of the specimen holder.

capping polymer without changing the particle shape? (2) What is the temperature at which the shape changes? (3) Is there a temperature-induced shape transformation due to surface diffusion? (4) What is the temperature at which the metallic crystal surface begins to melt, i.e., the temperature at which the liquid and solid metal coexist? (5) What is the value of the surface tension at the solid–liquid interface at this temperature?

The answers to these questions regarding the thermal properties of Pt nanocrystals are obtained by in-situ transmission electron microscopy (TEM). The shapes of the individual nanocrystals as well as their agglomerations are examined as the temperature increases from room temperature to  $\sim 700$  °C. The observed changes suggest that the capping polymer is removed between 180 and 250 °C. Significant truncation to nearly spherical shapes occurs near 500 °C. This temperature is just before surface melting, which occurs above 600 °C. The nanocrystals are transformed into a spherical-like shape by melting of the first few atomic layers of the surface. This gives a particle with a liquid layer surrounding a solid core. The large reduction in the melting temperature of the nanocrystals as

compared to the bulk platinum is shown to result from the formation of the solid–liquid interface surface tension ( $\gamma_{SL}$ ). The  $\gamma_{SL}$  is calculated at 650 °C for 8 nm diameter nanocrystals as  $2.0 \text{ N m}^{-1}$ . This value is lower than that of the bulk solid–vapor surface tension ( $\gamma_{SV}$ ), which is given in the literature<sup>4</sup> as between 2.6 and  $3.5 \text{ N m}^{-1}$ . This decrease is attributed to the wetting of the solid core surface atoms with the liquid layer, thus increasing the number of Pt–Pt bonds in comparison to the atoms at the crystal surface. Therefore, the wetting of the solid surface has a greater effect on the surface tension than the curvature of the nanocrystals.

## 2. Experimental Section

Pt nanocrystals with an average diameter of 8 nm were prepared by using the technique of Rampino and Nord<sup>5</sup> and Henglein et al.<sup>6</sup> Briefly, Ar gas was bubbled through the aged solution of  $\text{K}_2\text{PtCl}_4$ , which was adjusted to an initial pH of  $\sim 7$ , and reduced by flowing  $\text{H}_2$  gas. The starting ratio of  $\text{K}_2\text{PtCl}_4$  to polyacrylate (MW 2100) was 1:1, with the initial concentra-

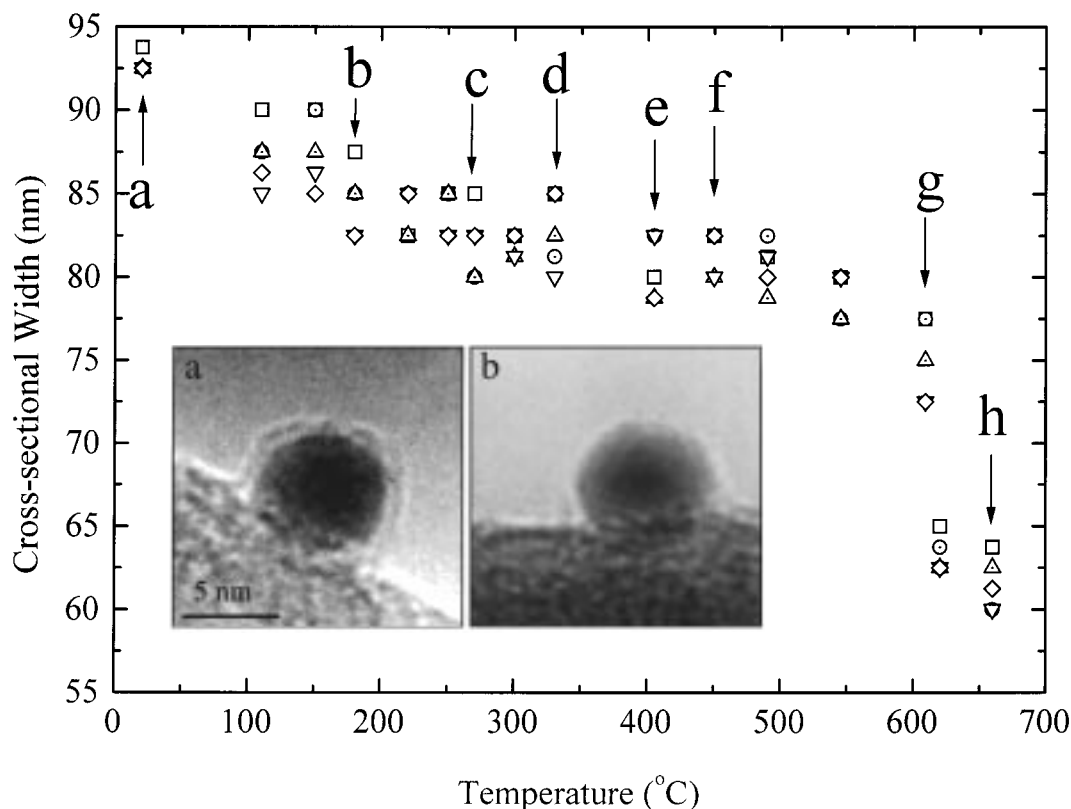


**Figure 2.** A plot of the agglomeration width of the TEM images shown in Figure 1 as a function of temperature. The first drop is observed in (b) at 180 °C, which is attributed to the capping polymer dissociation. Another small drop is observed in (g) at 610 °C, and a much larger decrease is observed in (h) at 660 °C, which is attributed to the melting of the agglomeration of the Pt nanocrystals. (Inset) In-situ TEM images recorded (a) at room temperature and (b) after annealing to 270 °C, showing the desorption of the capping polymer on the Pt nanocrystal.

tion of  $K_2PtCl_4$  being  $8 \times 10^{-5}$  M. The TEM grids were prepared for imaging by placing a small drop of the specimen solution on an ultrathin amorphous carbon film supported by a copper grid and allowing it to dry completely in air at ambient temperature.

Specimens with mixed cubic and tetrahedral shapes were chosen for the studies reported here in order to observe the shape transformation of Pt nanocrystals with different shapes in the same image. The in-situ TEM experiments were carried out at 200 kV using a Hitachi HF-2000 TEM, equipped with a field emission source. The specimen was annealed from room temperature to  $\sim 700$  °C using a Gatan TEM specimen heating stage, and the image was recorded using an CCD camera with a short exposure time (0.5 s) to minimize the effect introduced by thermal drift. The column pressure was kept at  $< 5 \times 10^{-8}$  Torr during the experiments.

The temperatures given here were sensed using a thermocouple attached to the furnace. The local temperature at the specimen region where the TEM observation was performed can be slightly different when the decay of heating and the beam-heating effect in the TEM are taken into consideration. Thus, an estimated uncertainty of  $\pm 15$  °C should be allowed.

This study mainly concentrates on cubic and tetrahedral nanocrystals. A cubic particle is bounded by six large  $\{100\}$  faces, although truncated  $\{111\}$  corners and  $\{110\}$  faces have been seen.<sup>2b</sup> The arrangement of the atoms on the surfaces and in the particle can be imaged in profile using TEM. A tetrahedral particle is enclosed by four  $\{111\}$  faces, and some truncation at the corners is also possible. The cubic and tetrahedral nanocrystals are ideal for studying the  $\{100\}$  and  $\{111\}$  face-dependent catalytic properties of Pt, respectively,

because both surfaces have very different crystallographic as well as electronic structure.<sup>7</sup>

### 3. Results

Tetrahedral, cubic, and truncated octahedral are the most frequently observed<sup>1</sup> particle shapes for Pt nanocrystals. Tetrahedral and cubic particles were chosen to examine the shape-induced transformation by temperature increase in the present study. The following sections are divided according to the observed changes as the temperature increases.

**3.1. Vaporization of the Capping Polymer on the Pt Nanocrystals.** To observe the loss of the capping polymer, two different types of experiments were carried out. In the first experiment, we examined regions in which the nanocrystals were agglomerated (the images shown in Figure 1). In comparison with the image recorded at 25 °C (Figure 1a), the width of the agglomeration decreased when the temperature reached  $\sim 180$  °C (Figure 1b). The shrinkage of the agglomeration width was measured by plotting this cross-sectional width vs temperature (25 to 660 °C) and is given in Figure 2. The letters correspond to the images in Figure 1. The widths were measured and plotted as five separate trials to account for any error in the measurements. A drop in the width of  $\sim 3$  nm is observed on going from (a) room temperature to (b) 180 °C. The shrinkage of the agglomeration is most likely due to the vaporization of the capping polymer between the particles and the rearrangement of Pt nanocrystals located on the top of the first layer adjacent to the substrate. Another apparent decrease that is observed in Figure 1 is the interparticle distance between the two individual nanocrystals, which is indicated by the arrowhead. These results suggest that the capping polymer evaporates at temperatures as low as 180 °C, thus bringing the particles closer together.

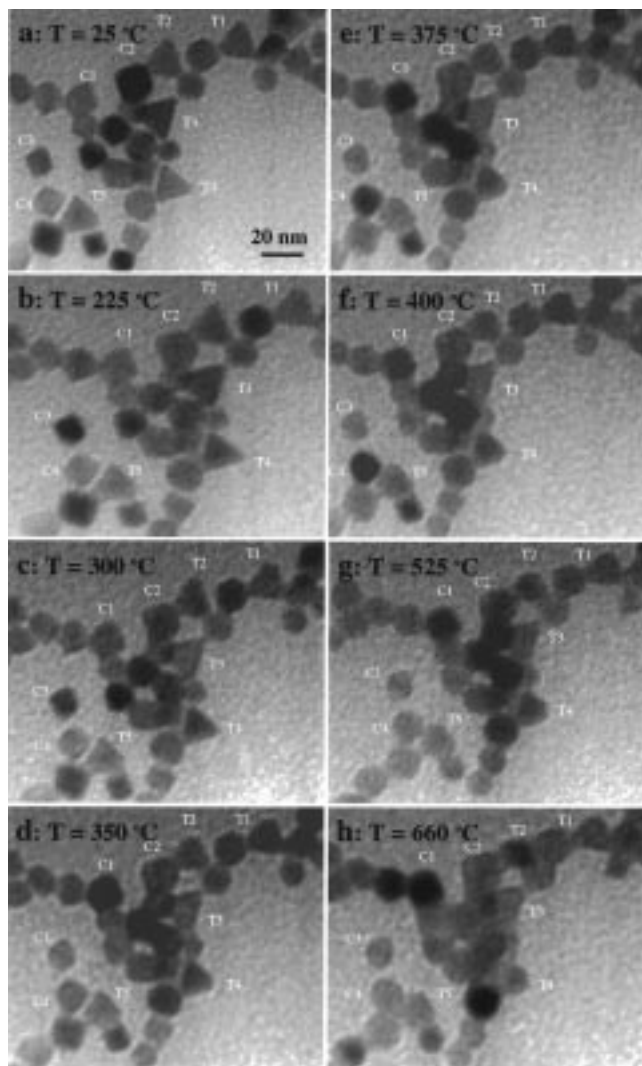


**Figure 3.** In-situ TEM images recorded from an area of the capped Pt nanocrystals at various specimen temperatures, showing the shape transformation and melting of individual Pt nanocrystals (see text).

To carefully observe the polymer dissociation on individual nanocrystals, the second experiment was carried out in which the Pt particles were dispersed on surfaces of large carbon spheres supported by a holey carbon film. This also enabled us to determine the temperature at which the surface-capping polymer was completely removed. The particles on the surfaces of the carbon spheres can be imaged in profile in TEM, so that the passivating surface polymer can be seen by phase contrast imaging without the influence of the substrate. The insert in Figure 2 shows an as-prepared Pt particle at room temperature before annealing (a), where a thin organic molecular layer with a thickness  $\sim 1\text{--}1.3$  nm is seen. After the specimen was heated to 270 °C, the surface-capping layer had been removed (b).

**3.2. Shape Transformation of the Pt Nanocrystals.** Figure 3 shows a series of TEM images recorded from the same region when the specimen temperature was increased from 25 to 660 °C. A few cubic (C1 to C4) and tetrahedral (T1 to T5) nanocrystals are labeled to trace their shape transformation behavior. Most of the particle shapes showed no significant change when the specimen temperature was below 300 °C (Figures 3a–c). Truncated cubic (C1–C4) and tetrahedral (T1, T2, T4, and T5) particles were formed when the temperature was increased to 350 °C (Figure 3d). This is evident by the disappearance of corners and edges of the particles. This is also consistent with the individually labeled particles in Figure

1. The truncation occurring from  $\sim 200\text{--}500$  °C does not seem to have a great effect on the size of the agglomeration in Figure 1, as is evidenced in the plot of Figure 2.

The tetrahedral particles could still be identified when the temperature reached 525 °C (Figure 3g), while the cubic particles became spherical-like when the temperature reached above 500 °C (Figure 3g,h). Therefore, tetrahedral particles seem to be more stable than the cubic ones. A striking feature observed in Figure 3 is that the tetrahedral shape of the T3 particle was preserved without truncation when the specimen temperature was as high as 525 °C. This is possibly due to the contact of the apexes of the T3 particle with the adjacent particles.

The small circles in Figure 4 show the changes in a group of TEM images illustrating the shape transformation of some individual Pt nanoparticles with temperature. The particle shapes showed significant truncation when the temperature reached 350 °C, as is shown in the region enclosed by the small circles. Further heating to 500 °C resulted in a dramatic change in particle shape (Figure 4c). Also shown in this figure by the small circles is the shrinking in the size of the individual particles.

The observed changes in the individual nanoparticle sizes in Figures 1, 3, and 4 could be induced by surface diffusion, which would lead to a three-dimensional atomic rearrangement, or possibly by surface sublimation. Atomic surface diffusion leading to changes in the observed image projection is energetically the most favorable.

**3.3. Coalescence and Melting of the Agglomerated Pt Nanocrystals.** After the removal of the polymer shown in Figure 1, the agglomeration of the nanocrystals preserved nearly the same configuration from 270 to 545 °C (Figures 1c–f and Figure 2). This was because the coalescence and significant surface melting had not occurred although surface diffusion was taking place (of course surface diffusion could be a result of surface premelting). Between 545 and 610 °C, a large change in the width as well as the total volume of the sample of the agglomerated nanocrystals is observed, as shown in both the images of Figure 1f,g and the plot of Figure 2. This is a strong indication of surface melting of this group of nanocrystals. This is further shown in the group of nanocrystals within the large circles of Figure 4. Some interparticle coalescing occurs at a temperature of 500 °C. At 610 °C, islands of connected particles are formed, which is indicated by the larger areas of red in the image. The clusters at this temperature retain a crystalline core as shown in the diffraction patterns from the same aggregate of nanocrystals before and after being annealed in-situ from 25 to 650 °C in Figure 5. Thus, at the high-temperature range, coexistence between the core solid and the liquid outside shell is observed.

#### 4. Discussion and Conclusions

The following is a summary of the in-situ TEM experiments, depicting the four distinct stages of nanocrystal shape transformation and surface melting. The as-synthesized Pt nanocrystals are capped with polymer, which can be removed when the specimen temperature is in the range of 180–250 °C. The particle shape shows no truncation until the temperature reaches  $\sim 350$  °C. Above 500 °C, the particle shape is dramatically changed to a spherical-like shape. The surface atoms can either diffuse on the surface and between different nanocrystals, or they can sublime. Energetically, surface diffusion requires far less energy. Between 600 and 660 °C, surface melting occurs at the first few atomic layers of the nanocrystals causing the

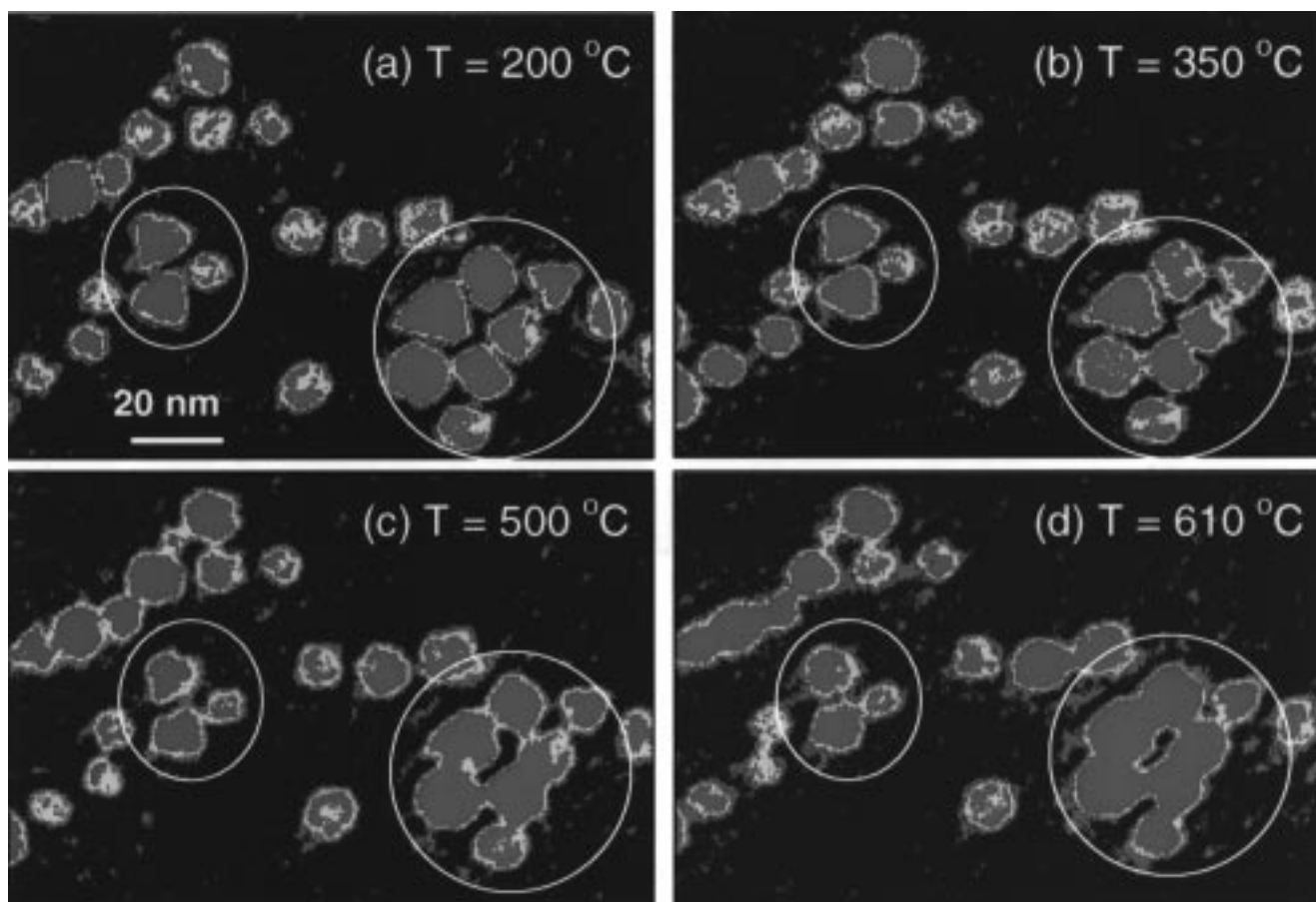


**Figure 4.** In-situ TEM images recorded from a region of capped Pt nanocrystals at various specimen temperatures. The images are color-enhanced to show the distinctive changes in particle shapes in the region encircled by a small circle and the melting for the group of nanocrystals encircled with the large circles. The blue color represents the substrate background, red depicts the approximate highest projected platinum atomic density, and yellow is the approximate lowest project platinum atomic density (see text).

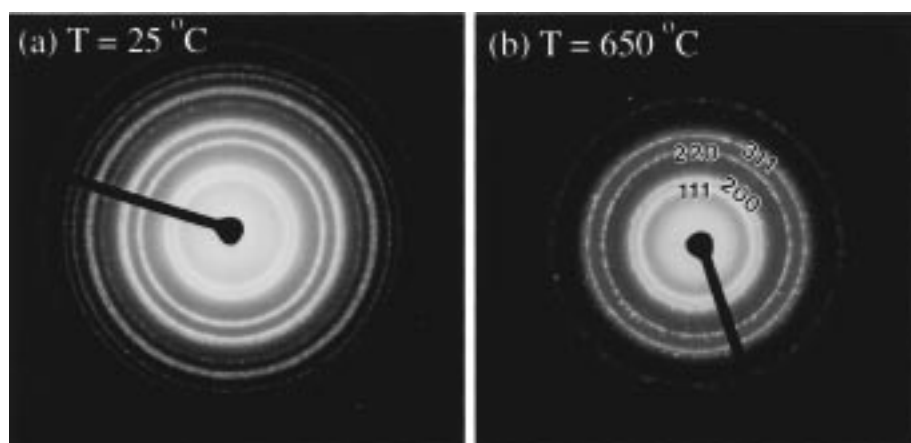


**Figure 5.** Diffraction pattern of the Pt nanocrystal sample at 25 and 650 °C.

formation of a spherical-like shape and/or the coalescence with close neighbors.

Our observations of the changes occurring in the Pt nanocrystals upon increasing temperature show that shape and relative orientation of neighboring particles affect truncation and surface melting. Nanoparticles that have their apexes stabilized by interactions with other nanocrystals retain their shapes at higher temperatures (see T3 in Figure 3). This interaction reduces their surface tension, and the added stabilization prevents them from undergoing surface diffusion. The higher temperatures at which truncation is observed for tetrahedral particles ( $T = 525$  °C) indicates that they are more stable than

the cubic ones ( $T = 500$  °C). This may be because the  $\{111\}$  surfaces are lower in energy than the  $\{100\}$ .<sup>6</sup> This might also have a kinetic origin as the tetrahedral geometry is more difficult to transform into spheres (the shape with the least surface tension) than the cubic shape. These studies also show that macroscopic melting of agglomerated nanocrystals starts at 600 °C, which is much lower than the melting point of bulk Pt (1769 °C at 1 atm pressure).<sup>9</sup>

Our results provide answers to the questions raised in section 1. First, by dispersing Pt particles evenly on the surface of a substrate without the presence of agglomerated regions, the capping polymer can be removed by annealing the specimen at

a temperature of 180–250 °C. This procedure is likely to produce activated Pt particles with well-preserved particle shapes, allowing for efficient catalytic activity. Second, the particle shape shows almost no change if the specimen temperature is lower than 350 °C. At a temperature between 350 and 450 °C, slight truncation takes place. Therefore, the resulting Pt particles can still be useful for studying shape-dependent properties if the reaction temperature is below ~450 °C. The particle shape experiences a dramatic transformation into a spherical-like shape when the temperature is higher than ~500 °C, possibly due to surface diffusion and/or sublimation. The carbon substrate has a large effect on the mobility of the nanocrystals on the surface, largely prohibiting the coalescence of the individual nanocrystals.

The issue of small clusters melting has been discussed previously in the literature.<sup>8–26</sup> Solid–liquid coexistence in these clusters is discussed using the capillarity approximation by Reiss, et al.<sup>8</sup> and by Buffat and Borel.<sup>11</sup> In our study, surface melting occurs and a surface solid–liquid core coexistence starts after the particle shape becomes near spherical and is best observed as the surface of neighboring particles begins to coalesce (e.g., the large circle in Figure 4) at 500 °C. At 610 °C, more surface melting has taken place as evidenced by the presence of more atoms found between the particles than at lower temperatures (500 °C). The core in these particles remains crystalline as shown in the diffraction patterns at different temperatures in Figure 5. In this figure, two diffraction patterns were recorded from the same aggregate of nanocrystals before and after being annealed in-situ from 25 to 650 °C. The intensities of the high index reflections (at high scattering angles) drop dramatically. This is due to the increased Debye–Waller factor from the atomic vibrations and the disordering of the atoms in the nanocrystals. Also, there are sharp spots in the pattern recorded at 650 °C, suggesting the formation of larger-size crystals due to the combination of nanocrystals. Finally, the total diffraction intensity at 650 °C is significantly lower than that at 25 °C, indicating the decrease in crystallinity of the nanocrystals. All of these facts support that the nanocrystals are experiencing a surface melting process at 650 °C.

It is clear that surface melting at 650 °C occurs at much lower temperatures than the melting point of the bulk (1769 °C).<sup>9</sup> According to Buffat and Borel,<sup>11</sup> the ratio of the melting temperature of the cluster ( $T$ ) with a radius  $r$  to that of the bulk ( $T_0$ ) is given by

$$\frac{T}{T_0} = -\frac{2}{\rho_S \lambda} \left[ \frac{\gamma_{SL}}{r - \delta} + \gamma_L \left( 1 - \frac{\rho_S}{\rho_L} \right) \right] \quad (1)$$

where  $\gamma_{SL}$  is the solid–liquid surface tension and  $\gamma_L$  is the surface tension of the liquid,  $\delta$  is the liquid layer thickness,  $\rho_S$  and  $\rho_L$  are the densities of the bulk solid and liquid, respectively, and  $\lambda$  is the heat of fusion. The equation derived by Reiss et al.<sup>8</sup> is essentially the same, but the liquid layer thickness term does not appear. Since the difference in the liquid and solid densities<sup>27</sup> is less than 2%, the last term in eq 1 is neglected. Using this approximation, one gets an expression for  $\gamma_{SL}$  from eq 1 to be

$$\gamma_{SL} = 1 - \frac{T}{T_0} \left[ r - \delta \left( \frac{\rho_S \lambda}{2} \right) \right] \quad (2)$$

As the temperature increases, the liquid layer begins to form on the surface of the nanocrystal. At 650 °C, the liquid layer thickness is estimated to be approximately 25%. Since the Pt

nanocrystals in these samples average 4 nm in radius,  $\delta$  is equal to 1 nm, corresponding to the first few atomic layers of the spherical surface. From this equation,  $\gamma_{SL}$  is estimated to be 2.0 N m<sup>-1</sup>. As the temperature continues to increase,  $\delta$  also increases (and  $r$  decreases), and  $\gamma_{SL}$  becomes 0 as the entire particle turns into liquid and the surface interface disappears.

Owing to the increase in the curvature of the nanoparticle, the solid–vapor surface tension,  $\gamma_{SV}$ , would normally increase when compared to that of the bulk<sup>4</sup>  $\gamma_{SV}$ , which is between 2.6 and 3.5 N m<sup>-1</sup>. However, the calculation is not for the outermost surface, but that of the interface between the two phases present. Therefore, the decrease of the  $\gamma_{SL}$  can be attributed to the increase in the total number of bonds formed by the solid surface atoms (in comparison to the atoms on the surface) owing to the wetting with the surrounding liquid layer. This wetting, and subsequent bond formation, more than compensates for the increase of  $\gamma_{SV}$  due to the large curvature of the nanoparticle.

Finally, two points need to be mentioned. First, the macroscopic values were used in eq 1 for the heat of fusion and the density. Upon heating the nanoparticle, the density and the heat of fusion are expected to decrease. The change in these terms would further decrease the value of  $\gamma_{SL}$  from that calculated above. Second, as was shown recently by Petroski et al.,<sup>28</sup> the particle shape at room temperature is determined by the kinetics of their formation (and not by the thermodynamics). Above 200 °C, each shape strives to be as near spherical in shape as possible in order to decrease the surface tension and attain the most thermodynamically stable configuration. This can be accomplished initially by surface diffusion and finally by surface melting.

**Acknowledgment.** This work was supported by the National Science Foundation Grants CHE-9727633 and DMR-9733160.

## References and Notes

- (1) Ahmadi, T.; Wang, Z. L.; Green, T. C.; Henglein, A.; El-Sayed, M. A. *Science* **1996**, *272*, 1924.
- (2) (a) Ahmadi, T.; Wang, Z. L.; Henglein, A.; El-Sayed, M. A. *Chem. Mat.* **1996**, *8*, 1161. (b) Wang, Z. L.; Ahmadi, T.; El-Sayed, M. A. *Surf. Sci.* **1997**, *380*, 302.
- (3) (a) Clint, J. H.; Collins, I. R.; Williams, J. A.; Robinson, B. H.; Towey, T. F.; Cajean, P.; Khan-Lodhi, A. *Faraday Discuss. Chem. Soc.* **1993**, *95*, 219. (b) Freund, P. L.; Spiro, M. *J. Phys. Chem.* **1985**, *89*, 1074.
- (4) Solliard, C.; Flueli, M. *Surf. Sci.* **1985**, *156*, 487.
- (5) Rampino, L. D.; Nord, F. F. *J. Am. Chem. Soc.* **1942**, *63*, 2745.
- (6) Henglein, A.; Ershov, B. G.; Malow, M. *J. Phys. Chem.* **1995**, *99*, 14129.
- (7) (a) Follstaedt, D. M. *Appl. Phys. Lett.*, **1993**, *62*, 1116. (b) Eaglesham, D. J.; White, A. E.; Feldman, L. C.; Moriya, N.; Jacobson, D. C. *Phys. Rev. Lett.* **1993**, *70*, 1643.
- (8) Reiss, H.; Mirabel, P.; Whetten, R. L. *J. Phys. Chem.* **1988**, *92*, 7241.
- (9) *Handbook of Chemistry and Physics*, 52nd ed.; The Chemical Rubber Co.: Boca Raton, FL, 1971.
- (10) Reiss, H.; Wilson, I. B. *J. Colloid Sci.* **1948**, *3*, 551.
- (11) Buffat, P.; Borel, J. P. *Phys. Rev. A* **1976**, *13*, 2287.
- (12) Goldstein, A. N.; Echer, C. M.; Alivasatos, A. P. *Science* **1992**, *256*, 1425.
- (13) Peppiat, S. J.; Sambles, J. R. *Proc. R. Soc. London, Ser.* **1975**, *A345*, 387.
- (14) Hahn, M. Y.; Whetten, R. L. *Phys. Rev. Lett.* **1988**, *61*, 1190.
- (15) Sheng, P.; et al. *J. Phys. C* **1981**, *14*, L565.
- (16) Solliard, C.; *Surf. Sci.* **1981**, *106*, 58.
- (17) Coombes, C. J. *J. Phys. F* **1972**, *2*, 441.
- (18) Pawlow, P. Z. *Phys.* **1909**, *66*, 549.
- (19) Brian, C. L.; Burton, J. J. *J. Chem. Phys.*, **1975**, *63*, 2045.
- (20) Berry, R. S.; Jellinek, J.; Natanson, G. *Phys. Rev. A*, **1984**, *30*, 919.

- (21) Kristensen, W. D.; Jensen, E. J.; Cotterill, R. M. *J. Chem. Phys.* **1974**, *11*, 4161.
- (22) Honeycutt, J. D.; Andersen, H. C. *J. Chem. Phys.* **1987**, *91*, 4950.
- (23) Hanzen, K. J. *Z. Phys.* **1960**, *157*, 523.
- (24) Hasegawa, M.; Hoshino, K.; Watabe, M. *J. Phys.* **1980**, *10*, 619.
- (25) Wronski, C. R. *J. Appl. Phys.* **1967**, *18*, 1731.
- (26) Cleveland, C. L.; Landmann, U.; Luedtke, W. D. *J. Phys. Chem.* **1994**, *98*, 6272.
- (27) Zinov'ev, V. E.; *Handbook of Thermophysical Properties of Metals at High Temperatures*; (Nova Science Publishers; New York, 1996; p 345.
- (28) Petroski, J. M.; Wang, Z. L.; Green, T. C.; M. A. El-Sayed, *J. Phys. Chem. B* **1998**, *102*, 3316.